Syntheses, Structures, and Mesomorphism of a Series of Cu(II) Salen Complexes with 4-Substituted Long Alkoxy Chains

Y. Abe

N. Nakazima

T. Tanase

Department of Chemistry, Faculty of Science, Nara Women's University, Kitauoya-Nishimachi, Nara 630-8506, Japan

S. Katano

H. Mukai

K. Ohta

Department of Functional Polymer Science, Faculty of Textile Science & Technology, Shinshu University, Ueda 386-8567, Japan

Abstract

A series of copper(II) salen complexes containing 4-substituted alkoxy chains of aromatic rings, [Cu((4-$C_nH_{2n+1}O)_2$salen)] (*n* = 3 (**1**), 4 (**2**), 6 (**3**), 8 (**4**), 10 (**5**), 12 (**6**), 14 (**7**), 16 (**8**), 18 (**9**), and 20 (**10**)) and salen=*N, N'*-ethylenebis(salicylideneiminato)) has been prepared and single crystal structures of **2**・H_2O, **4**, and **6** by an X-ray crystallographic analysis have been revealed. Complexes **4** and **6** form tetrahedrally distorted square planer structure with one-dimensional polymeric stacking by van der Waals interaction between the dramatically distorted salen moieties. Complexes **1** - **3** did not exhibit any mesophases, but complexes **4**–**10** with longer alkoxy chains of *n*=8–20 showed the metallomesogen of a lamello-columnar (ColL) mesophase in the smectic layers with the nearly constant stacking distances,

irrespective of the variation of the alkoxy chain lengths by the X-ray diffraction measurements, which show similar behaviors to the corresponding Ni(II) complexes of *n*=14-20. The molecular assemblies and mesomorphic properties in relation to the single crystal structures of **4** and **6** with the liquid crystals at higher temperature are discussed.

Keywords

Cu(II) complexes, salen ligand with 4-substituted long alkoxy chains, crystal structure, metallomesogen

INTRODUCTION

Liquid crystals with transition-metal core groups, called as metallomesogens, have attracted increasing attention because of the possibility of combining their physico-chemical properties of the metal (color, magnetism, polarizability, redox behavior, etc) with those of organic framework [1-5]. Since the metallomesogens are achieved through changes of molecular conformation, shape, and structure, their physico-chemical properties can be turned by the choice of metal ions, substituents, and position of substituents on core moieties [6-8]. Schiff base ligands provide a wide range of ways to modify liquid crystal compounds [9-15]. However, to date there has been no systematic investigation concerning molecular assemblies and metallomesogens of metal-salen (salen=*N,N′*-ethylenebi(salicylidene-iminato)) complexes substituted by two long alkoxy chains at the 4-positions though the metal-salen complexes with 5-substituted alkoxy or alkyl chains usually show smectic A (S_A) mesophases at higher temperature [11-15]. In the previous papers, we prepared two series of the VO(IV) and Ni(II) salen complexes with two long alkoxy chains introduced at the 4-positions, [VO((4-$C_nH_{2n+1}O)_2$salen)] [16-17] and [Ni((4-$C_nH_{2n+1}O)_2$ salen)] [18] (*n*=3–20), and found new mesomorphism of the VO(IV) salen complexes with *n*=16–20 , which was unambiguously elucidated in relation to the bilayer crystal structure assembled by the

VO(IV) complex. The Ni(II) salen complexes with longer alkoxy chains of n=14–20 showed an unusual metallomesogen of a lamello-columnar (ColL) mesophase. For the Ni(II) complexes, in the absence of diffraction quality crystals for any of the longer alkoxy chains ($n \geqq 14$) homologues, the parent complex [Ni((4-OH)$_2$saen)] and [Ni((4-$C_6H_{13}O$)$_2$salen)] could be considered as model compounds and molecular assemblies taken as being representative for the discussion of the liquid crystal states of similar mesomorphic complexes. In the present work, a series of Cu(II) salen complexes with two 4-substituted long alkoxy chains, [Cu((4-$C_nH_{2n+1}O$)$_2$salen)] (n = 3 (**1**), 4 (**2**), 6 (**3**), 8 (**4**), 10 (**5**), 12 (**6**), 14 (**7**), 16 (**8**), 18 (**9**), and 20 (**10**)) has been prepared and fortunately, the single crystal structures of **4** and **6** with the mesomorphism at higher temperature have been revealed by an X-ray crystallographic analysis. The structures in liquid crystalline state with the ColL mesophase have been affiliated with the molecular assemblies in the crystalline states. The comparisons of the Cu(II) and Ni(II) complexes with the ColL mesophase [18] are discussed. There are few reports on the metallomesogen of the ColL mesophase [19-21].

EXPERIMENTAL

Reagents and Measurements

All chemicals and solvents for the synthesis were used without further purification of reagent grade. Organic solvents of superfine reagent grade were dried over molecular sieves prior to use for the spectroscopic measurements and cyclic voltammetry measurements. Electronic absorption and infrared spectra were recorded on Shimadzu UV-240 spectrophotometer and JASCO FT/IR-8900μ in KBr media, respectively. Hokuto Denko HZ-1A apparatus was used for cyclic voltammetry measurements. The measurements were carried out in CH_2Cl_2 solution containing n-Bu_4NClO_4 (0.1 mol dm^{-3}) as a supporting electrolyte with a three-electrode cell including a platinum working electrode, a platinum counter electrode, and an

Ag/Ag^+ reference electrode. The mesomorphic nature of the complexes has been studied using polarized optical microscopy equipped with a thermoregulator-controlled heating plate as well as with a Mettler FP980 and a FP82HT, and measured with differential scanning calorimetry on a Shimadzu DSC-50 and a Rigaku Thermoplus TG-8120. The temperature-dependent X-ray diffraction was measured using a Rigaku RAD with Cu*K*α radiation equipped with a thermoregulator-controlled heating plate [22].

Synthesis of [Cu((4-$C_nH_{2n+1}O)_2$salen)] ((*n* = 3 (1), 4 (2), 6 (3), 8 (4), 10 (5), 12 (6), 14 (7), 16 (8), 18 (9), and 20 (10))

Ethylenediamine (3.0 g, 0.050 mol) was added to a solution of 2,4-dihydroxybenzaldehyde (13.8 g, 0.10 mol) in methanol (150 mL) and stirred at 60 ℃ for 2 h. The obtained (4-$OH)_2$salenH_2 was collected and washed with diethyl ether. A mixture of (4-$OH)_2$salenH_2 (27 g, 0.090 mol) and $Cu(CH_3COO)_2 \cdot H_2O$ (19.0 g, 0.095 mol) in the presence of CH_3COONa in ethanol (150 mL) was stirred at room temperature for 24 h. The preciptated [Cu((4-$OH)_2$salen)](**11**) was filtered off and washed with ethanol, and diethyl ether. The reaction of **11** (3.6 g, 10 mmol) with BrC_nH_{2n+1} (*n* = 3, 4, 6, 8, 10, 12, 14, 16, 18, or 20) (40 mmol) in the presence of K_2CO_3 in DMF (100 - 200 mL) for several days afforded [Cu((4-$C_nH_{2n+1}O)_2$salen)] (*n* = 3 (**1**), 4 (**2**), 6 (**3**), 8 (**4**), 10 (**5**), 12 (**6**), 14 (**7**), 16 (**8**), 18 (**9**), or 20 (**10**)). After evaporation of solvent, dark violet precipitate was isolated by filtration, washed with methanol and diethyl ether. Crude complexes were purified by passing a silica-gel column with eluents of CH_2Cl_2 : MeOH (20–25 : 1 (v/v)). Elemental Anal. Calc. for $C_{22}H_{26}N_2O_4Cu \cdot H_2O$ (**1**) (446.02): C, 56.96, H, 6.08, N, 6.04. Found: C, 59.90; H, 6.05; N, 6.01%. Yield 70 %. Calc. for $C_{24}H_{30}N_2O_4Cu$ (**2**) (474.06): C, 60.81; H, 6.38; N, 5.91. Found: C, 60.90; H, 6.30; N, 5.85 %. Yield 70 %. Calc. for $C_{28}H_{38}N_2O_4Cu$ (**3**) (530.17): C, 63.43, H, 7.22, N, 5.28. Found: C, 63.16; H, 7.19; N, 5.24 %. Yield 60 %. Calc. for $C_{32}H_{46}N_2O_4Cu$ (**4**)

(586.28): C, 65.56, H, 7.91, N, 4.78. Found: C, 65.42; H, 7.86; N, 4.81 %. Yield 60 %. Calc. for $C_{36}H_{54}N_2O_4Cu$ (**5**) (642.39): C, 67.16, H, 8.43, N, 4.31. Found: C, 67.31; H, 8.47; N, 4.36 %. Yield 50 %. Calc. for $C_{40}H_{62}N_2O_4Cu$ (**6**) (698.49): C, 68.78, H, 8.95, N, 4.01. Found: C, 68.65; H, 8.89; N, 3.99 %. Yield 40 %. Calc. for $C_{44}H_{70}N_2O_4Cu$ (**7**) (754.60): C, 70.04, H, 9.35, N, 3.71. Found: C, 69.73; H, 9.27; N, 3.67 %. Yield 30 %. Calc. for $C_{48}H_{78}N_2O_4Cu$ (**8**) (810.71): C, 71.11, H, 9.70, N, 3.46. Found: C, 70.68; H, 9.59; N, 3.41 %. Yield 20 %. Calc. for $C_{52}H_{86}N_2O_4Cu$ (**9**) (866.82): C, 72.05, H, 10.00, N, 3.23. Found: C, 71.89; H, 9.93; N, 3.21%. Yield 15 %. Calc. for $C_{56}H_{94}N_2O_4Cu$ (**10**) (922.92): C, 72.34, H, 10.35, N, 2.83. Found: C, 72.88; H, 10.27; N, 3.04 %. Yield 10 %.

X-ray Crystallographic Analyses

Single crystals of **2** • H_2O, **4**, and **6** suitable for X-ray crystallography were obtained from the slow evaporation of CH_2Cl_2 solutions. The crystal data and experimental conditions are summarized in Table 1. All data were collected at –120 °C on a Rigaku/MSC Mercury CCD diffractometer equipped with graphite-monochromated Mo*Ka* radiation using a rotating-anode X-ray generator. A total of 2160 oscillation images, covering a whole sphere of $2\theta < 55$ °, were collected with exposure rates of 128 sec/^{o} by the ω scan method ($-62 < \omega < 118$ °) with $\Delta\omega$ of 0.25 °. The crystal-to-detector (70 x 70 mm) distance was set to 60 mm. The data were processed using the Crystal Clear 1.3.5 program (Rigaku/MSC) [23(a)] and corrected for Lorentz-polarization and absorption effects. The structures of **2** • H_2O, and **4** and **6** were solved by direct methods (SIR92) [23(b)] and Patterson method (DIRDIF PATTY), respectively, and refined on *F* with the full-matrix least-squares techniques using the teXsan crystallographic software package [23(c)]. All non-hydrogen atoms were refined with anisotropic thermal parameters, and the positions of the hydrogen atoms were calculated with C-H = 0.95 Å and fixed in the refinement. All calculations

were carried out on a Silicon Graphics O2 workstation running teXsan and on a Pentium-based PC running the Crystal Structure package [23(d)].

RESULTS AND DISCUSSION

Synthesis and Characterization

The stoichiometry and purity of all complexes were confirmed using elemental analyses, UV-vis and IR spectroscopies, and cyclic voltammetry (CV). Single crystal X-ray analysis of [Cu((4-$C_nH_{2n+1}O)_2$salen)] (**2** · H_2O (n = 4), **4** (n = 8), and **6** (n = 12) was performed. The UV-vis spectra of **1**-**11** exhibit d-d transitions (λ_{3max}) in addition to strong metal-to-metal charge transfer (LMCT) bands (λ_{2max}) and n-π transitions in the ligand (λ_{1max}) (Table 2). Since cyclic voltammogram (CV) showed the irreversible Cu(III)/Cu(II) couples, the values of the oxidation waves (E_{ox}) are summarized in Table 2. The data of UV-vis and cyclic voltammogram (CV) are approximately constant regardless of the variation of the alkoxy chain lengths in a series of the Cu(II) complexes. IR data were similar to those of [Ni((4-$C_nH_{2n+1}O)_2$salen)] [18].

Crystal structures of 2 · H_2O (n = 4), 4 (n = 8), and 6 (n = 12)

Molecular structures and crystal packings of **2** · H_2O and **6** are shown in Figure 1 (a) and (b), and Figure 2 (a) and (b), respectively, and those of **4** are deposited in Figure 3. The selected bond distances and angles, and dihedral angles are summarized in Table 3. Complex **2** · H_2O forms an extremely distorted square-pyramidal structure by the apical coordination of the H_2O molecule to the Cu metal center with dihedral angles of 18.744^o between the basal N_2O_2 plane and aromatic rings (Figure 1(a)). The Cu atom is displaced by 0.1898 Å from the N_2O_2 plane toward apical oxygen atom of H_2O. On the basis of the Jahn-Teller effect, the apical Cu–O3 distance (2.296 Å) is longer than the Cu-O (1.944 Å) and Cu-N (1.959 Å) distances

in the basal N_2O_2 plane. On the other hand, [Cu(salen)] exists as dimers intermolecularly bridged through phenoxo oxygen atoms between the Cu atoms, forming the pair-wise link by two Cu and two O atoms [24-25]. Copper adopts tetragonally distorted square-pyramidal structure. The Cu atom is displaced by 0.14 Å toward the bridging oxygen atom with asymmetrical dihedral angles of 24.9 ^{o} and 3.1 ^{o} between the N_2O_2 plane and aromatic rings [25]. While two Cu-N distances (1.958 Å) are equal, two Cu-O distances (1.945 Å and 1.911 Å) show significant difference in the N_2O_2 plane. The apical (bridged) Cu-O distance (2.414 Å) is longer than those of the basal plane as well as that of **2** · H_2O. The significant difference of the bond distances and dihedral angles between **2** · H_2O and [Cu(salen)] is due to the monomer for **2** · H_2O and the dimer for [Cu(salen)] in a distorted square-pyramidal structure, depending on the presence and absence of the substituents at the 4-positions of aromatic rings. On the other hand, in the case of [Ni(salen)], the structure forms face-to-face dimer separated by 3.08 Å with weak π–π stacking which is not intermolecularly bridged between the phenoxo oxygen atoms and the Ni atoms [26]. The difference of these structures may be due to the preference of the square planar structure of [Ni(salen)] as compared to [Cu(salen)].

Molecular structure and crystal packing of **4** resemble to those of **6** (Figures 2 and 3). Complex **4** and **6** have tetrahedrally distorted square planar structure composed of the significantly distorted salen moieties with dihedral angles of 23.856 ^{o} and 23.829 ^{o} between the basal N_2O_2 plane and aromatic rings, respectively. The Cu atom sites at 0.2511 Å and 0.2931 Å from the N_2O_2 plane for **4** and **6**, respectively. The Cu-O (1.905–1.906 Å) and Cu-N (1.931–1.934 Å) distances are relatively short in comparison to those of **2** · H_2O and [Cu(salen)]. This difference is based on a square planar structure for **4** and **6** as contrast with a square-pyramidal structure for **2** · H_2O and [Cu(salen)]. The molecular packings of **4** and **6** are consisted of the face-to-face structure by one-dimensional polymeric stacking

formed by van der Waals interaction of ca. 3.3–3.5 Å (Cu(1)···C(3)=3.305 Å, Cu(1)···C(2)=3.311 Å, C(1)···C(4)=3.514 Å, O(1)···C(2)=3.350 Å) between the distorted salen moieties with the Cu–Cu distance of 4.8162 Å and 4.9061 Å, respectively (Figures 2 and 3). On the other hand, in the crystal of the Ni(II) complex with two alkoxy chains (*n*=6) at the 4 potisions, two molecules (**A**, **B**) with slightly different bond distances and angles are present [18]. Two aromatic rings of **A** or **B** are not coplanar to each other with the dihedral angles of 14.501° and 7.764° (**A**) or 13.468° and 8.158° (**B**) relatively smaller than those of **4** (23.856 °) and **6** (23.829 °). Moreover, the molecules are organized by a set of weak C-H···O type hydrogen bonded interaction between neighboring molecules with a dihedral angle of 59.570° between the N_2O_2 plane of **A** and the N_2O_2 plane of **B**. The stacking leads to one-dimensional structure with the Ni-Ni distance of 5.994 Å.

In the solid states of [Cu((5-$CH_3O)_2$salen)] with 5-substituted alkoxy groups, the molecules form weak dimeric structure as well as [Cu(salen)] [25]. The Cu atom is displaced by only 0.06 Å toward the bridging phenoxo oxygen atom with smaller asymmetrical dihedral angles of 14.5 ° and 9.9 ° than those of [Cu(salen)]. The apical (bridged) Cu-O distance (2.801 Å) is relatively long in comparison of that (2.414 Å) of [Cu(salen)]. On the other hand, the dimeric structure of [Cu((5-$C_6H_{13}O)_2$salen)]·$CHCl_3$ is the co-planar to each other between the N_2O_2 plane and aromatic rings [27]. Moreover, the dimeric structure consists of isolated molecules with weak pair-wise link between the Cu atoms and the alkoxy oxygen atoms at the 5-positions (3.53 Å) of the adjacent molecules. The molecular pairs so formed are further linked into pseudo-polymeric chains by weaker (4.01 Å) interactions of the outer alkoxy oxygens with the Cu atoms of adjacent pairs. Thus, the geometry and assembly for [Cu((4-$C_nH_{2n+1}O)_2$salen)] (*n*=8, 12), and [Cu((5-$C_6H_{13}O)_2$salen)]·$CHCl_3$ depend significantly on the positions of substituents on the aromatic rings, leading to the different mesomorphic properties at higher temperature as described

below.

Mesomorphic properties of 4 (*n*=8) –10 (*n*=20)

The mesomorphic nature of complexes has been studied by three methods using polarized optical microscopy, differential scanning calorimetry (DSC), and temperature-dependent X-ray diffraction (XRD) measurements [28]. From these measurements, complexes **1** – **3** did not exhibit the mesomorphic property. On the other hand, the crystalline phases for **4** – **10** were transformed into phases with mosomorphic nature. The natural texture of **10 (***n*=20**)** is shown in Figure 4. Figure 4 shows the X-ray patterns for the enantiotropic mesophase of **7** (*n*=14) at 140 ^{o}C by XRD measurements as one example, which are very similar to the X-ray patterns of the planar Ni(II) complexes of *n*=14–20 with a lamello-columnar (ColL) mesophase [18] rather than those of the pyramidal VO(IV) complexes of *n*=16–20 [16-17]. X-ray patterns have three arrow reflections (No. **1**–**3**) in the low-angle region blow 10^{o} and their spacing in a ratio of 1:1/2:1/3 which correspond to the (001), (002), and (003) planes with a lamellar distance *c* (Figure 5 and Table 5). A diffuse band around 20^{o} (No. **5**) is due to the melting of alkoxy chains. With these reflections, the X-ray pattern possesses an additional peak at 14^{o} (No. **4**), indicating that the X-ray pattern for this mesophase affords the stacking distance in a columnar structure in addition to the lamellar structure. Thus, this mesophase has both lamellar and columnar structures corresponding the lamello-columnar (ColL) mesophase with a stacking distance *h* in the *a* axis direction. The stacking distances *h*=6.02 – 6.12 Å for **5** –**10** are independent of the variation of the alkoxy chain lengths. This stacking distances well correspond to the distance between the inter-molecules with the alkoxy chains in the same direction. Thus, the stacking distances between the monomers are attributed to be ca. 3 Å. The lamellar distance *c* with 25.5 – 41.2 Å for **5**–**10** is linear to the number of carbon atoms in the alkoxy chain (*n*) with the slope of 1.56 (Figure 6), which may tilt toward the layer. Hence,

schematic representation of the ColL mesophase of **5** – **10** can be illustrated as Figure 7. The Ni(II) complexes with *n*=10–20 exhibit the similar behaviors to the CuII) complexes which show the lamello-columnar mesophase. The *h* values for the Cu(II) complexes are a slightly smaller than those (6.20–6.24 Å) for the Ni(II) complexes, but the slope of the lamellar distances is a slightly larger than that of the Ni(II) complexes with 1.44. If the Miller index of (100) were not present in this mesophase, this mesophase would be regarded as the smectic mesophase. The ColL mesophase possesses an unusual columnar phase with the one-dimensional ordering of molecules within the smectic layers. There are few reports on the metallomesogen of the ColL mesophase [19-21]. For the ColL mesophase with the linear rod-like molecules, the distance attributed to the stacking between the aromatic rings in the monomers was measured directly as *ca*. 3.4 Å [21]. In the case of the Cu(II) complexes, the absence of the peak attributed to *ca*. 3.4 Å may depend on the structure of the Cu(II) complex with 4-substituted alkoxy groups with the U-shaped structure without the linear rod-like structures.

The X-ray crystal structures for **4** and **6** can be available for the discussion on the liquid crystal states since **4** and **6** show the mesomorphic property at high temperature. The molecular assemblies of the prototypes of the complexes exhibit notable features when the crystalline phase transforms into the liquid crystalline phase [17, 27]. The molecular packing of **6** is consisted of one-dimensional polymeric stacking formed by van der Waals interaction of 3.3–3.5 Å with the face-to-face between the salen cores as described above (Figure 2). When this crystal is transferred into the liquid crystal, the stacking distance in the liquid crystal shows ca 3 Å slightly smaller than 3.3-3.5 Å. This result suggests that the change from the dramatically distorted salen moieties in the crystal to the almost planer salen moieties in this ColL mesophase occurs at higher temperature above 130 ^{o}C, leading to the more approach of the distance between the salen moieties. Thus, the stacking distance with ca. 3 Å

at higher temperature may be adequate to this ColL structures. The apical (bridged) Cu-O distance in dimer for [Cu(salen)] is 2.414 Å considerably shorter than ca. 3 Å. The Cu-Cu distance may be longer than ca. 3 Å as shown in Figure 7.

Phase transition temperatures and enthalpy changes for [Cu((4-$C_nH_{2n+1}O)_2$salen)] (n=3–20) obtained by DSC measurements are summarized in Table 4. All the complexes exhibit the appearance of the isomeric crystal phases during the formation of isotropic liquid. The dependence of the number of carbon atoms in the alkoxy chain (n) for the 4-alkoxysalen on the phase transition temperature is shown with the data for [Ni((4-$C_nH_{2n+1}O)_2$salen)] [18] in Figure 8. The transition temperature from the crystalline phase or the ColL mesophase to isotropic liquid (I.L.) decreases gradually upon increasing the number of carbon atoms (n) in accordance with the Ni(II) homologues. However, the occurrence of the ColL mesophase of [Cu((4-$C_nH_{2n+1}O)_2$salen)] exhibits at the alkoxy chain lengths shorter than that of [Ni((4-$C_nH_{2n+1}O)_2$salen)]. This may be due to the difference of the molecular packings as described in above section. For **5** – **10**, the enthalpy changes (ΔH_{clear} = 23.3– 25.2 kJ mol^{-1}) from the liquid crystal phase ColL to I.L. at the clearing point are approximately independent of the alkoxy chain lengths (Table 4). The ΔH_{clear} values are comparable to those of [Ni((4-$C_nH_{2n+1}O)_2$salen)] (n=14–20) (ΔH_{clear}=23.9–25.5 kJ mol^{-1}). Though the occurrence of the ColL mesophase of [Cu((4-$C_nH_{2n+1}O)_2$salen)] exhibits at the alkoxy chain lengths shorter than that of [Ni((4-$C_nH_{2n+1}O)_2$salen)], similar enthalpy changes are based on the structure of the ColL mesophase with similar stacking distances of the Cu(II) and Ni(II) complexes irrespectveof the variation of the alkoxy chain lengths, because the enthalpy changes from the ColL mesophase to I.L. are generated from the rupture of the polymeric stacking between the cores. The enthalpy changes at the clearing point are considerably larger than these observed for the complexes with the shorter alkyl or alkoxy chains at the 5-position with the S_A mesophase of the linear rod-like (1D) structure [9-15]. Because **5** – **10** with two longer alkoxy

chains at the 4-positions exhibit ColL mesophase which shows the more ordered 2D rectangular mesophase than the S_A mesophase of the linear rod-like (1D) structure. The enthalpy changes increase as the order in the mesophase increases because the interaction between the neighboring core groups is large in the 2D rectangular mesophase compared to the S_A mesophase of the 1D structure [29]. Chipperfield *et al*. have reported (5-substituted troporonato)copper(II) complexes with aloxy chains with 18.42 kJ/ mol for n = 10 and 26.80 kJ /mol for n = 16 in the transformation from isotropic liquid to the S_B phase [27]. Furthermore, in general, complexes with the larger molecular weight and/or long alkoxy or alkyl chains exhibit larger enthalpy changes for the transition between phases [19(b), 27].

The Co(II), Ni(II), Cu(II), and VO(IV) salen complexes with 5-substituted alkoxy or alkyl chains of the aromatic rings usually show smectic A (S_A) mesophases at higher temperature because of the linear rod-like (1D) crystal structures. The [Ni((5-C_6H_{13})$_2$salen)] complex transforms enantiotropically from dimer-smectic E (S_E) at lower temperature to monomer-S_A mesophases at higher temperature [15]. However, new series of [VO((4-$C_nH_{2n+1}O$)$_2$salen)] (n =16–20) and [Cu((4-$C_nH_{2n+1}O$)$_2$salen)] (n=8–20) in addition to [Ni((4-$C_nH_{2n+1}O$)$_2$salen)] (n=14–20) with two alkoxy long chains introduced at 4-positions exhibit new mesophase M(Pa2$_1$) [16-17] and the ColL mesophase with the linear stacking structure [18], respectively. These liquid crystal structures are closely related with the molecular assemblies in the crystalline state when the crystalline phase transfers into the liquid crystalline phase.

CONCLUTION

Single crystal structures of **2**・H_2O, **4**, and **6** by an X-ray crystallographic analysis have been revealed. The molecular assemblies and mesomorphic properties of the Cu(II) complexes with the ColL mesophase are affiliated with the single crystal structures of **4** and **6** with the mesomorphism at higher temperature. Since in contrast to the Cu(II) and Ni(II) complexes,

the VO(IV) complexes with the square-pyramidal structure forms the mesophase M(Pa2_1) with the bilayer structure from the bilayer crystal structure, the assemblies and the mesomorphic properties depend remarkably on the selection of the metal ions and the positions of substituents on aromatic rings of salen moieties.

ACKNOWLEDGEMENTS

We are grateful to the Nara Women's University Intramural Grant for Project Research.

SUPPLEMENTALY MATERIALS

Crystallographic data for the structures reported in this paper are deposited with Cambridge Crystallographic Data center as supplementary publication No. CCDC 607247-607249.

REFERENCES

*Author to whom correspondence should be addressed. E-mail: yabe@cc.nara-wu.ac.jp, TEL/FAX: +81-742-20-3394.

[1] B. Donnio, D. W. Bruce, in *Structure and Bonding*, (Ed.: D. M. P Mingos), Vol. 95, *Liquid Crystals II. Metallomesogens*, Springer (1999). (b) B. Donnio, D Guillon, R. Deschenaux, D. W. Bruce, *"Metallomesogens" in Comprehensive Coordination Chemistry II.* Vol. 6 (Eds.: J. A. McCleverty, T. J. Meyer), Elsevier: Oxford (2003)

[2] A-M. Giroud-Godquin, P. M. Maitlis, *Angew. Chem. Int. Ed. Engl.*, **30**, 375 (1991).

[3] M. H. Chisholm, *Acc. Chem. Res.,* **33,** 53 (2000).

[4] P. Kirsch, M. Bremer, *Angew. Chem. Int. Ed. Engl.*, **39**, 4216 (2000).

[5] I. Aiello, M. Ghedini, M. La Deda, D. Pucci, O. Francescangeli, *Eur. J. Inorg. Chem.,*

1367 (1999).

[6] (a) D. Pucci, G. Barberio, A. Crispini, O. Francescangeli, M. Ghedini, *Mol. Cryst. Liq. Cryst.,* **395**, 325 (2003). (b) G. Barberio, A. Bellusci, A. Crispini, M. Ghedini, A. Golemme, P. Prus, D. Pucci, *Eur. J. Inorg. Chem.,* 181 (2005).

[7] X-H. Liu, M. N. Abser, D. W. Bruce, *J. Organomet. Chem*., **551**, 271 (1998).

[8] A. B. Blake, J. R. Chipperfield, W. Hussain, R. Paschke, E. Sinn, *Inorg. Chem*., **34**, 1125 (1995).

[9] N. Hoshino, H. Murakami, Y. Matsunaga, T. Inabe, Y. Maruyama, *Inorg. Chem*., **29,** 1177 (1990).

[10] (a) R. Paschke, H. Zaschke, A. Maedicke, J. R. Chipperfield, A. B. Blake, P. G. Nelson, G. W. Gray, *Mol. Cryst. Liq. Cryst. Lett*., **6**, 81 (1988). (b) T. D. Shaffer, K. A. Sheth, *Mol. Cryst. Liq. Cryst*., **172**, 27 (1989). (c) R. Paschke, D. Balkow, U. Baumeister, H. Hartung, J. R. Chipperfield, A. B. Blake, P. G. Nelson, G. W. Gray, *Mol. Cryst. Liq. Cryst*. **188**, 105 (1990).

[11] R. Paschke, S. Diele, I. Letko, A. Wiegeleben, G. Pelzl, K. Grieser, M. Athanassopoulou, W. Haase, *Liq. Cryst*., **18**, 451 (1995).

[12] R. Paschke, D. Balkow, E. Sinn, *Inorg. Chem*., **41**, 1949 (2002).

[13] (a) A. Serrette, P. J. Carroll, T. M. Swager, *J. Am. Chem. Soc*., **114**, 1887 (1992). b) Additions and Corrections: A. Serrette, P. J. Carroll, T. M. Swager, *J. Am. Chem. Soc.*, **115**, 11656 (1993).

[14] A. G. Serrette, T. M. Swager, *J. Am. Chem. Soc.*, **115**, 8879 (1993).

[15] (a) K. Ohta, Y. Morizumi, T. Fujimoto, I. Yamamoto, K. Miyamura, Y. Gohshi, *Mol. Cryst. Liq. Cryst.*, **214**, 161 (1992). (b) K. Miyamura, A. Mihara, T. Fujii, Y. Gohshi, Y. Ishii, *J. Am. Chem. Soc*. **117**, 2377 (1995).

[16] Y. Abe, K. Nakabayashi, N, Matsukawa, M. Iida, T. Tanase, M. Sugibayashi, H. Mukai,

K. Ohta, *Inorg. Chem. Commun*., **7**, 580 (2004).

[17] Y. Abe, K. Nakabayashi, N, Matsukawa, H. Takashima, M. Iida, T. Tanase, M. Sugibayashi, H. Mukai, K. Ohta, *Inorg. Chim. Acta*, **359**, 3934 (2006).

[18] Y. Abe, H. Akao, Y. Yoshida, H. Takashima, T. Tanase, H. Mukai, K. Ohta, *Inorg. Chim. Acta,* **359**, 3147 (2006).

[19] (a) J. Billard, *C. R. Acad. Sc. Paris.,* **299***,* 905 (1984). (b) K. Ohta, H. Muroki, A. Takagi, K. Hatada, H. Ema, I. Yamamoto, and K. Matsuzaki, *Mol. Cryst. Liq. Cryst*., **140**, 131 (1986).

[20] S. Mèry, D. Haristoy, J-F. Nicoud, D. Cuillon, S. Diele, H. Monobe, Y. Shimizu, *J. Mater. Chem.*, **12**, 37 (2002).

[21] A. El-ghayoury, L. Douce, A. Skoulios, R, Ziessel, *Angew. Chem. Int. Ed.,* **37**, 1255 (1998).

[22] H. Hasebe, Master Thesis, Shinshu University, Ueda, Japan, Chap. 5 (1991).

[23] (a) Crystal Clear 1.3.5: Operating software for the CCD detector system. Rigaku and Molecular Structure Corp. (2003). (b) A. Altomare, M. C. Burla, M. Camalli, M. Cascarano, C. Giacovazzo, A. Guagliardi, G. Polidori, *J. Appl. Cryst.,* **27**, 435 (1994). (c) TEXSAN: Crystal Structure Analysis Package, Molecular Structure Corp. (1999). (d) Crystal Structure 3.6: Crystal Structure Analysis Package, Rigaku and Molecular Structure Corp. (2003).

[24] E. N. Barker, D. Hall, T. N. Waters, *J. Chem. Soc. (A).,* 400 (1979); 406 (1979).

[25] M. M. Bhadbhade, D. Srinivas, *Inorg. Chem*., **32**, 6122 (1993).

[26] (a) F.F. Dimauro and M. C. Kozoiowski, *Organometallics,* **21**, 1454 (2003). (b) M. Kondo, K. Nabari, T. Horiba, Y. Irie, M. K. Kabir, R. P. Sarker, E. Shimizu, Y. Shimizu, Y. Fuwa, *Inorg. Chem. Commun*., **6**, 154 (2003). c) X. Cheng, S. Gao, L. Huo, S. W. Ng, *Acta. Cryst.*, **E61**, m385 (2005).

[27] (a) J. R.Chipperfield, S. Clark, J. Elliott, E. Sinn, *Chem. Commun*., 195 (1998). (b) J. M. Elliott, J. R. Chipperfield, S. Clark, *Inorg. Chem*., **41**, 293 (2002).

[28] F. Maeda, K. Hatsusaka, K. Ohta, M. Kimura, *J. Mater. Chem*., **13**, 243 (2003).

[29] (a) K. Pelz. W. Weissflog, U. Baumeister, S. Diele, *Liq. Cryst.*, **30**, 1151 (2003). (b) D. Kardas. M. Prehm, U. Baumeister, D. Pociecha, R. A. Reddy, G. H. Mehl, C. Tschierske, *J. Mater. Chem*., **15**, 1722 (2005).

TABLE 1 Crystallographic and Experimental Data for [Cu((4-$C_nH_{2n+1}O)_2$salen)](n = 4 (**2** · H_2O), 8 (**4**), 12 (**6**))

	2 · H_2O	**4**	**6**
Empirical formula	$C_{24}H_{32}CuN_2O_5$	$C_{32}H_{46}CuN_2O_4$	$C_{40}H_{62}CuN_2O_4$
Formula weight	492.07	586.27	698.49
Crystal Color	green blue	pale brown	pale brown
Crystal Dimens. / nm	0.45×0.30×0.10	0.40×0.35×0.05	0.35×0.15×0.05
Crystal System	orthorhombic	monoclinic	monoclinic
Space group	*P*nma(#62)	*C*2/c(#15)	*C*2/c(#15)
a(Å)	8.8753(4)	43.04(1)	52.569(4)
b(Å)	34.267(2)	7.211(2)	7.3513(5)
c(Å)	7.5402(2)	9.603(2)	9.7909(5)
β (deg)		92.642(1)	91.496(1)
V (Å^3)	2293.2(2)	2976(1)	3782.4(4)
Z	4	4	4
D_{calc}(g/cm^3)	1.425	1.308	1.226
μ (Mo-Kα) (cm^{-1})	9.9	7.72	6.18
2θ rang,deg	6-55	6-55	6-55
No.variables	149	178	214
No observation	2228 (I >2σ(I))	2966 (I >2σ(I))	2500 (I >2σ(I))
temp. (^{o}C)	-120	-120	-120
Residuals :*R;Rw*[a]	0.058; 0.133	0.061; 0.140	0.062; 0.163
GOF	1.08	1.16	1.13

[a] $R = \Sigma ||F_0| - |F_c|| / \Sigma |F_0|$. $R_w = \{[\Sigma w(F_0^2 - F_c^2)^2] / \Sigma [(w(F_0^2)^2)]\}^{1/2}$

TABLE 2 Absorption Maxima and E_{ox} Values for [Cu((4-$C_nH_{2n+1}O)_2$salen)] (n = 3 (**1**), 4 (**2**) , 6 (**3**) , 8 (**4**) , 10 (**5**) , 12 (**6**) , 14 (**7**) , 16 (**8**) , 18 (**9**) , and 20 (**10**) and [Cu((4-$HO)_2$ salen)] (**11**) in CH_2Cl_2

Complex	n	λ_{1max}/nm	log ε	λ_{2max}/nm	log ε	λ_{3max}/nm	log ε	E_{ox} / V vs. Ag-Ag^{+} [b]
1	3	292	4.459	351	3.983	566	2.623	0.61
2	4	292	4.513	351	4.016	564	2.638	0.62
3	6	292	4.428	351	3.954	564	2.609	0.61
4	8	292	4.477	349	4.010	566	2.602	0.62
5	10	292	4.480	349	3.983	566	2.634	0.63
6	12	292	4.476	351	3.981	566	2.615	0.63
7	14	290	4.506	351	4.034	566	2.622	0.63
8	16	290	4.450	351	4.005	566	2.603	0.62
9	18	290	4.449	351	3.973	566	2.612	0.63
10	20	292	4.501	349	4.004	566	2.601	0.62
11[a]	-	288	4.380	347	3.916	550	2.591	0.53

[a]DMF was used. [b]Scan speed : 100 mV /s.

TABLE 3 Selected Bond Distances (Å) and Angles (°), and Dihedral Angles (°) for

[Cu((4-$C_nH_{2n+1}O)_2$salen)] (n = 4 (**2** · H_2O), 8 (**4**), 12 (**6**))

	2 · H_2O	**4**	**6**
Cu-O1	1.944(2)	1.906(2)	1.905(3)
Cu-O1*	1.944(2)	1.906(2)	1.905(3)
Cu-N1	1.959(3)	1.931(2)	1.934(3)
Cu-N1*	1.959(3)	1.931(2)	1.934(3)
Cu-O3	2.296(3)		
O1-Cu-O1*	91.2(1)	92.8(1)	92.1(2)
O1-Cu-N1	91.9(1)	94.63(8)	94.6(1)
O1-Cu-N1*	168.1(1)	160.46(8)	161.7(1)
O1*-Cu-N1	168.1(1)	160.46(8)	161.7(1)
O1*-Cu-N1*	91.9(1)	94.63(8)	94.6(1)
O3-Cu-O1	95.20(8)		
O3-Cu-O1*	95.20(8)		
O3-Cu-N1	96.0(1)		
O3-Cu-N1*	96.0(1)		
O1-O1*-N1*-N1 and C4-C5-C6-C7-C8-C9	18.744	23.856	23.829
O1-O1*-N1*-N1 and C4*-C5*-C6*-C7*-C8*-C9*	18.744	23.856	23.829

TABLE 4 Phase Transition Tenperature and Enthalpy Changes for [Cu((4-$C_nH_{2n+1}O)_2$salen)] (n=3 (**1**), 4(**2**) , 6 (**3**), 8 (**4**), 10 (**5**) , 12 (**6**) , 14 (**7**) , 16 (**8**) , 18 (**9**) , and 20 (**10**))[a]

Complex	n	Phase $\xrightarrow[[\Delta H\ (\text{kJ/mol})]]{T(^{o}\text{C})}$ Phase	Relaxation
1	3	$K_1 \xrightarrow{112.7\ [14.1]} K_2 \xrightarrow{155.2\ [4.44]} K_3 \xrightarrow{208.9\ [21.1]}$	I.L.
2	4	$K1 \xrightarrow{89.8\ [15.1]} K2 \underset{}{\overset{208.5\ [17.5]}{\rightleftharpoons}}$	I.L.
3	6	$K_1 \xrightarrow{60.2\ [11.6]} K_2 \underset{}{\overset{113.8\ [1.53]}{\rightleftharpoons}} K_3 \underset{}{\overset{182.4\ [20.0]}{\rightleftharpoons}}$	I.L.
4	8	$K_1 \underset{}{\overset{75.0\ [14.6]}{\rightleftharpoons}} K_2 \underset{}{\overset{182.3\ [29.2]}{\rightleftharpoons}}$	I.L.
		$\overset{181.6}{\rightsquigarrow}$ ColL ⇄ I.L. (Rapid cooling)	
5	10	$K_1 \xrightarrow{74.2\ [4.19]} K_2 \underset{}{\overset{108.5\ [8.78]}{\rightleftharpoons}} \text{ColL} \underset{}{\overset{165.1\ [24.5]}{\rightleftharpoons}}$	I.L.
6	12	$K_1 \underset{}{\overset{81.7\ [21.7]}{\rightleftharpoons}} \text{ColL} \underset{}{\overset{157.7\ [23.3]}{\rightleftharpoons}}$	I.L.
7	14	$K_1 \xrightarrow{47.8\ [1.08]} K_2 \underset{}{\overset{100.2\ [47.0]}{\rightleftharpoons}} \text{ColL} \underset{}{\overset{155.5\ [25.2]}{\rightleftharpoons}}$	I.L.
8	16	$K_1 \xrightarrow{36.8\ [19.1]} K_2 \underset{}{\overset{98.6\ [57.4]}{\rightleftharpoons}} \text{ColL} \underset{}{\overset{151.6\ [25.2]}{\rightleftharpoons}}$	I.L.
9	18	$K1 \xrightarrow{96.7\ [99.0]} \text{ColL} \underset{}{\overset{146.0\ [25.0]}{\rightleftharpoons}}$	I.L.
		$K_3 \underset{}{\overset{66.3\ [12.0]}{\rightleftharpoons}} K_2 \underset{}{\overset{90.6\ [34.8]}{\rightleftharpoons}}$	
10	20	$K_1 \underset{}{\overset{94.4\ [47.9]}{\rightleftharpoons}} \text{ColL} \underset{}{\overset{141.9\ [23.7]}{\rightleftharpoons}}$	I.L.

[a]Phase nomenclature:K=crystal, M= mesophase and I.L.=isotropic liquid.

TABLE 5 X-ray Data for the Mesophase ColL of [Cu((4-$C_nH_{2n+1}O)_2$salen)] (n = 10 (**5**), 12 (**6**), 14 (**7**), 16 (**8**), 18 (**9**), 20 (**10**))

Complex	n	Lattice parameter	Peak No.	Spacing (Å)		Miller indices
				Observed	Calculated	(*h k l*)
5	10	*c*=25.5	1	25.5	25.5	(001)
		h=6.10	2	12.9	12.8	(002)
		at 160 °C	3	8.56	8.50	(003)
			4	6.10	-	(100)
			5	ca.4.7	-	#
6	12	*c*=29.4	1	29.4	29.4	(001)
		h=6.10	2	14.6	14.7	(002)
		at 150 °C	3	9.73	9.80	(003)
			4	6.10	-	(100)
			5	ca.4.7	-	#
7	14	*c*=32.2	1	32.2	32.2	(001)
		h=6.02	2	16.1	16.1	(002)
		at 140 °C	3	10.7	10.7	(003)
			4	6.02	-	(100)
			5	ca.4.7	-	#
8	16	*c*=35.6	1	35.6	35.6	(001)
		h=6.10	2	17.7	17.8	(002)
		at 140 °C	3	11.7	11.9	(003)
			4	6.10	-	(100)
			5	ca.4.5	-	#
9	18	*c*=38.4	1	38.4	38.4	(001)
		h=6.01	2	19.1	19.2	(002)
		at 140 °C	3	12.7	12.8	(003)
			4	6.01	-	(100)
			5	ca.4.5	-	#
10	20	*c*=41.2	1	41.2	41.2	(001)
		h=6.12	2	20.6	20.6	(002)
		at 130 °C	3	13.7	13.7	(003)
			4	6.12	-	(100)
			5	ca.4.5	-	#

#: Halo of the melton alkoxy chains.

Figure captions

FIGURE 1. (a) Molecular structures of **2** • H_2O. (b) Crystal packing diagram of **2** • H_2O, viewed along the c axis. Hydrogen atoms are omitted for clarity.

FIGURE 2. (a) Molecular structures of **6**. (b) Crystal packing diagrams of **6**, viewed along the *a* axis (b(1)) and down the *b* axis (b(2)). Hydrogen atoms are omitted for clarity. Dashed and solid lines indicate two different distances of Cu-Cu and the van der Waals interaction among the salen moieties, respectively.

FIGURE 3. (a) Molecular structures of **4**. (b) Crystal packing diagrams of **4**, viewed along the *a* axis (b(1)) and down the *b* axis (b(2)). Hydrogen atoms are omitted for clarity. Dashed and solid lines indicate two different distances of Cu-Cu and the van der Waals interaction among the salen moieties, respectively.

FIGURE 4. Polarized optical micrograph of the ColL mesophase of **10** (n = 20) at 130 ^{o}C on cooling the I.L. phase from 145 ^{o}C.

FIGURE 5. X-ray diffraction patterns of the ColL mesophases of **7 (** n **= 14)** at 140 ^{o}C.

FIGURE 6. The n (n = number of carbon atoms in the alkoxy chain) dependence of the lattice constants, h and c for the Cu(II) 4-alkoxysalen complexes.

FIGURE 7. Schematic representation of the ColL mesophase for [Cu((4-$C_nH_{2n+1}O)_2$salen)] (*n* = 10 (**5**), 12 (**6**), 14 (7), 16 (**8**), 18 (**9**), 20 (**10**)).

FIGURE 8. The *n* (*n* = the number of carbon atoms in the alkoxy chain) dependence of the phase transition temperature for the Cu(II) 4-alkoxysalen complexes (red) and Ni(II) 4-alkoxysalen complexes (black).

.

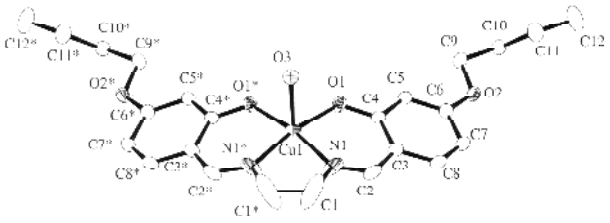

(1)

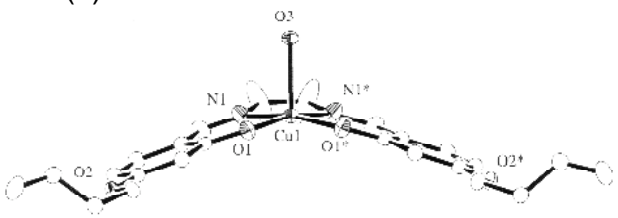

(2)

(a)

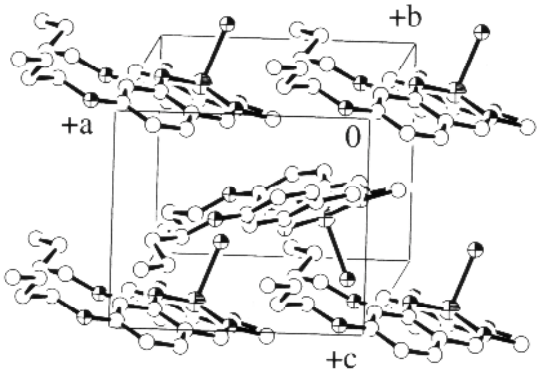

(b)

Figure. 1

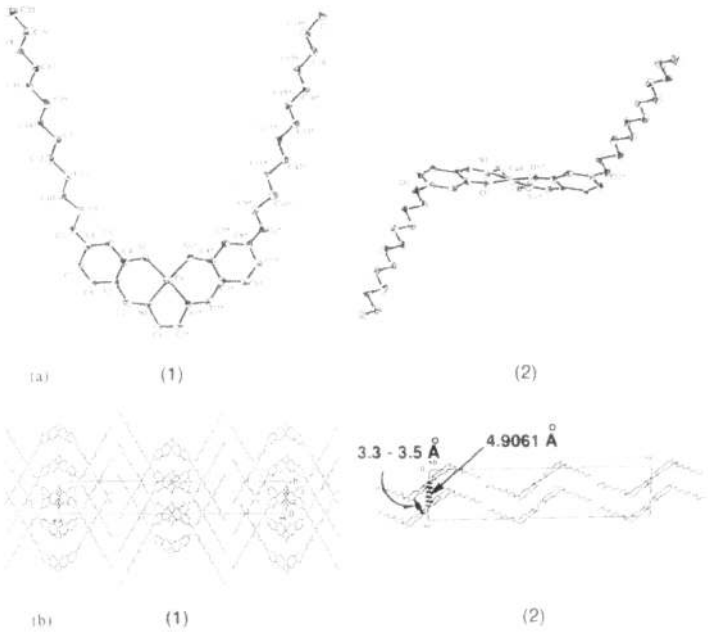

Figure 2

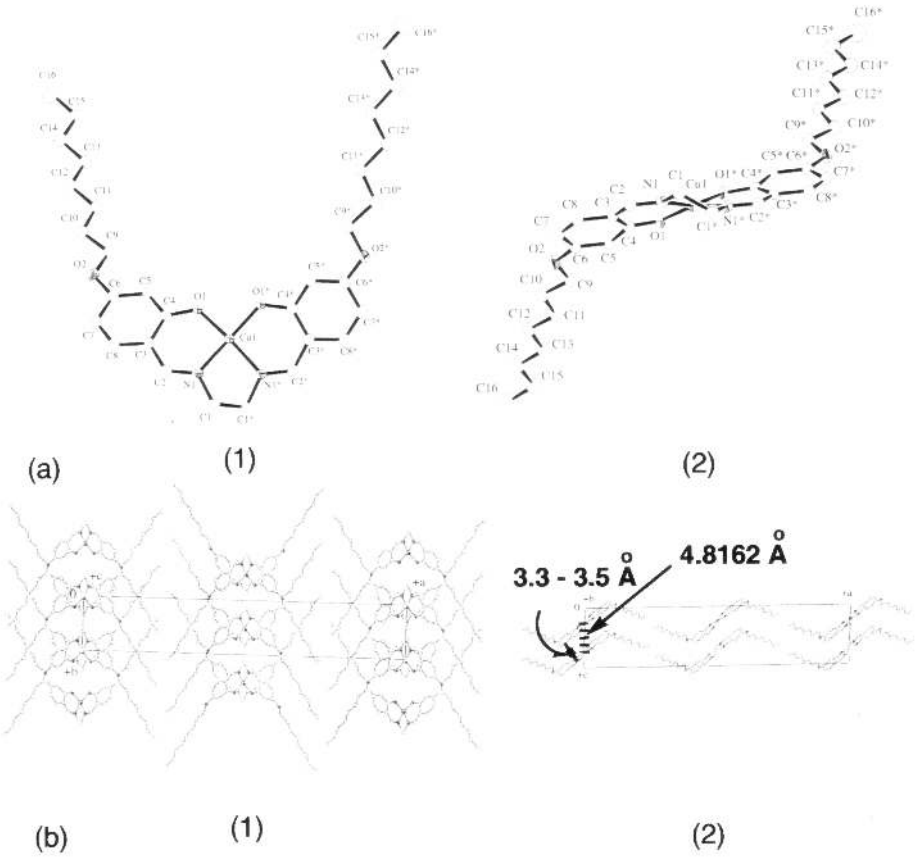

Figure 3

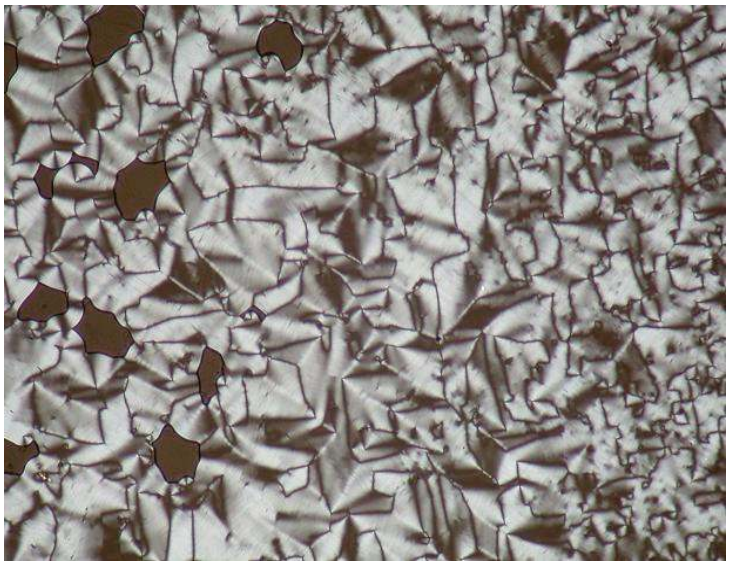

Figure 4

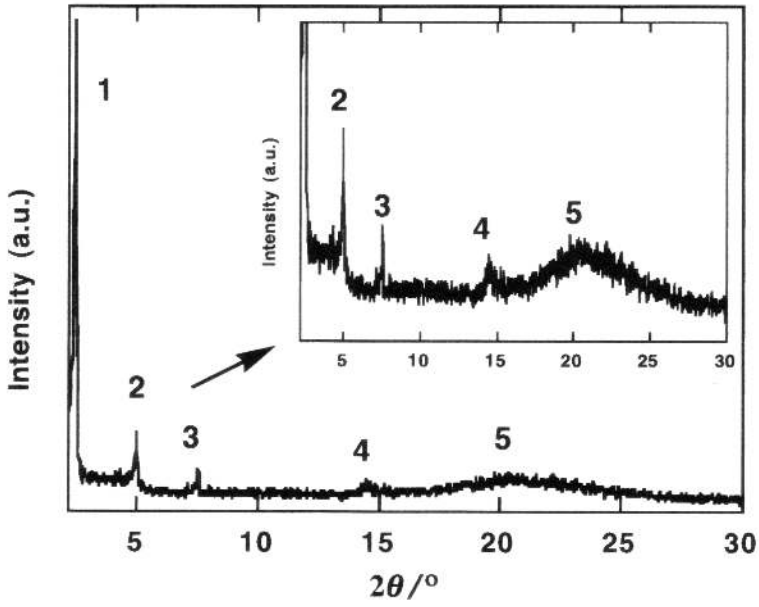
Intensity (a.u.)
1
2
3
4
5
5
10
15
20
25
30
2θ/°
Intensity (a.u.)
2
3
4
5
5
10
15
20
25
30

Figure 5

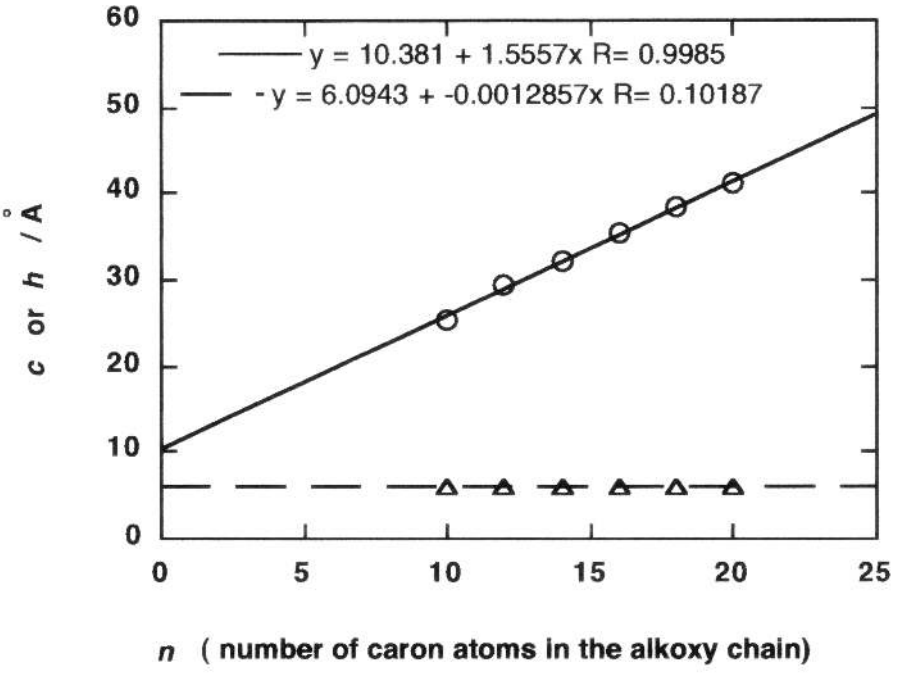
y = 10.381 + 1.5557x R= 0.9985
- y = 6.0943 + -0.0012857x R= 0.10187
c or h / Å
n (number of caron atoms in the alkoxy chain)
0
10
20
30
40
50
60
0
5
10
15
20
25

Figure 6

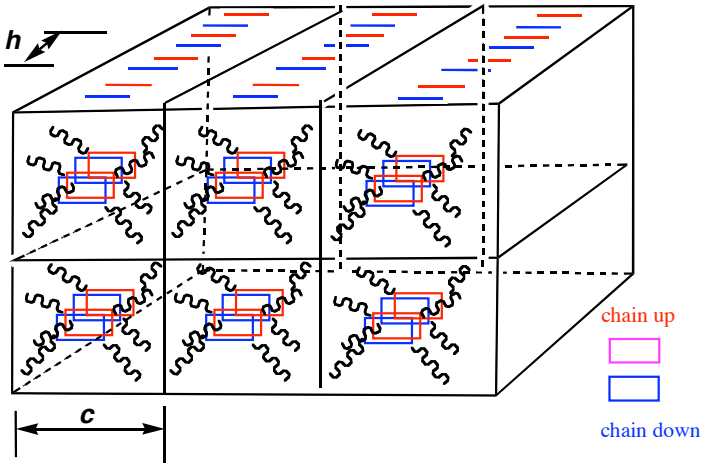

ColL Mesophase

Figure 7

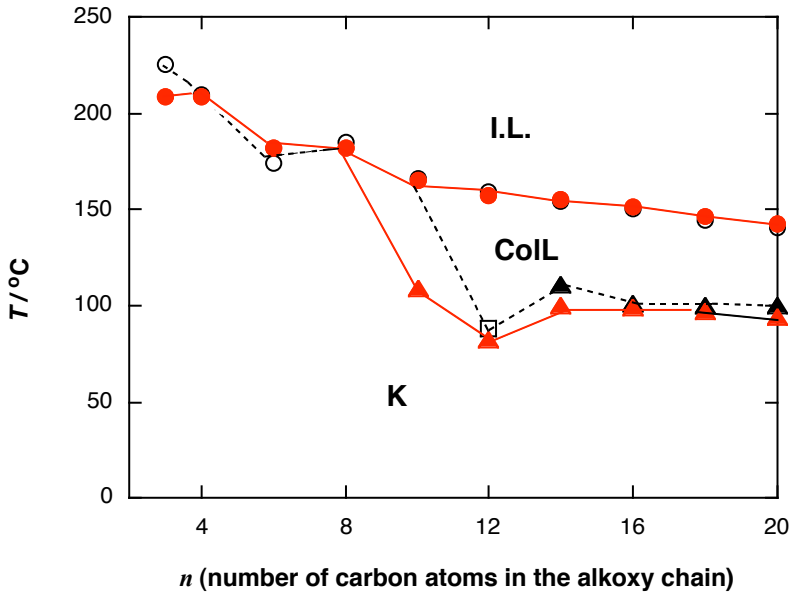
250
200
150
100
50
0
T / °C
I.L.
ColL
K
4
8
12
16
20
n (number of carbon atoms in the alkoxy chain)

Figure 8